Indian Journal of Fibre & Textile Research
Vol. 50, March 2025, pp. 99-105
DOI: 10.56042/ijftr.v50i1.4778

Comparative analysis of electrostatic filtration in pilot pulse-jet and flat-based test rigs

Sudev Dutta[1,a] , Arunangshu Mukhopadhyay[2], A K Choudhary[2] & C C Reddy[3]

[1]Lovely Professional University, Phagwara 144 411, India

[2]Department of Textile Technology, Dr B R Ambedkar National Institute of Technology, Jalandhar 144 011, India

[3]Department of Electrical Engineering, Indian Institute of Technology, Ropar 140 001, India

Received 10 August 2023; revised received and accepted 1 February 2024

This study investigates the filtration performance of three different filter media—PTFE (Polytetrafluoroethylene)-coated media, stainless steel fibre blended with PET (Polyethylene Terephthalate) media, and stainless steel fibre scrim media—under varying charge levels and dust concentrations using a pilot pulse-jet filter unit and a flat-based test rig. The effect of charge, material type, and dust concentration on filtration efficiency, particulate emissions, and charge dissipation behaviour is systematically examined. Results indicate that charge plays a dominant role in enhancing filtration efficiency by promoting dust agglomeration and improving dust cake properties. PTFE-coated media exhibits the lowest particulate emissions across both test rigs, whereas stainless steel fibre scrim media demonstrates the fastest charge dissipation. A comparative analysis reveals that the pilot pulse-jet filter unit exhibits higher particulate emissions than the flat-based test rig due to its non-uniform dust deposition and cleaning inefficiencies. The study further establishes strong correlations between downstream particulate emissions, mass concentration, and particle number concentration across the two test rigs. Findings provide valuable insights into optimising charge-assisted filtration mechanisms and understanding the influence of electrostatic charge on different filter media.

Keywords: Conductive media, Dust agglomeration, Mass concentration, Pulse-jet system, Pre-charger

1 Introduction

Electrostatically assisted hybrid systems have evolved as one of the most widely adopted aerosol collecting techniques in industrial applications due to their high mass collection efficiency and low-pressure drop with relatively low capital and operating costs[1-5]. Numerous studies[6,7] have been conducted on the performance of different hybrid system designs; however, there is still a dearth of research on comparing the filtration parameters of different types of conductive filter media, as all the reported studies were confined to keeping the filter media fixed mostly with either Polyphenylene sulfide (PPS) material or Teflon coated fabric. Industries employing electrostatically assisted filtration systems are prone to static charge accumulation, resulting in spark generation hazards. To mitigate this risk, conductive filter media have been introduced, consisting of conductive elements that dissipate the static charge. Besides the comparative analysis of different conductive filter materials, there lies a dearth of research on the comparative study of the effect of various dust charge levels on conductive materials' filtration behaviour. Another vital aspect significantly influencing the filtration behaviour of materials is inlet dust concentration. The amount of dust approaching the filter media significantly impacts the filter media's surface behaviour. Further, it was reported that for the same particle size, both average and average residual pressure drops are reduced with the decrease of maximum pressure, but both the number of pulse-jet cleaning and the average dust emission concentration are increased, which lowers the dust collection efficiency. The track of dust particles is affected by numerous mechanical mechanisms such as inertial impaction, interception, gravitational settling and Brownian motion. These mechanisms deposit the aerosol over the filter media and separate them from the exhaust gas[8,9]. It is also to be added that the emission behaviour of filter media also affects its life[10,11]. Early seepage and clogging can lead to reduced life filter media and its frequent replacement, eventually leading to high investment costs for the industries.

Some of the previous researches[12-14] have reported an enhanced filtration performance of filter materials through charging the aerosol particles. Studies on

[a]Corresponding author.
E-mail: Sudev89@gmail.com

varying dust densities and their effect on emission have also been carried out using varying particle size distribution dust[15]. However, to date, no comprehensive study has been reported on conductive filter media. Therefore, by considering the above-mentioned research gaps, the present study has been undertaken to analyse the effect of various charged and non-charged conditions on filtration and pressure drop behaviour of different types of conductive filter media under different inlet dust concentrations. The study's findings are expected to be beneficial in choosing the best conductive filter material that can be widely used in filtration industries under various operating conditions.

Furthermore, industrial filtration systems experience significant fluctuation in dust density, making it essential to assess the response of both test rigs across varying dust concentration levels. System design is immensely influenced by dust density; while lower dust concentration improves filtration performance (lower emission at the cost of lower energy and longer filtration life) at the cost of larger bag houses on the basis of air-to-cloth ratios. Thus, system designers must balance dust density and filter unit size to optimise performance and cost efficiency. The present research aims to analyse the effects of dust concentration under both uncharged and charged conditions and evaluate the interactions of these parameters.

2 Materials and Methods

Needle-punched nonwoven materials are generally preferred for pulse-jet filtration in industrial applications due to their ability to prevent direct particle penetration through intermeshed pores and their resilience against high-intensity shock during pulsing operations. Considering these factors, polyester needle-punched conductive filter materials were selected for this investigation. The material specifications are presented in Table 1.

The experimental investigation was conducted using two distinct laboratory-based pulse-jet filtration set-ups: a flat media test rig embedded with a pre-charger, where the filter media is in a flat rectangular form and a pilot filter unit, where the media is in a cylindrical bag shape. Generally, filter materials are tested in a flat form at the laboratory scale, while industrial applications employ a cylindrical bag form. Hence, in the present case, the pilot filter unit is closer to the real-time industrial situation. The reason for characterising the ageing performance of filter materials across these two set-ups was to analyse how their behaviour changes at a scaled-up level.

In a flat media test rig, the set-up comprised a dust feeder to ensure uniform dust feeding, followed by a pre-charger installed to charge the aerosol particles. A dust layer was created on the surface of filter media during filtration and was periodically dislodged using a pressure-based method at a peak pressure of 1000 Pa, with a pulsing time of 50 milliseconds. The downstream side was equipped with an online particle size analyser ‘Promo 2000’ to analyse the emitted particles. The standard followed was ISO 11057 and fly ash was used as the aerosol. The dimensions of flat specimen were 50 cm in length and 18 cm in width.

The operational mechanism for the pilot filter unit was similar to that of the flat media test rig, but the filter media was in a cylindrical bag form. Each filter bag measured 125 mm in diameter and 800 mm in height.

Testing conditions:

- Inlet face velocity: 2 m/min
- Air to cloth ratio: 2
- Inlet dust concentrations: 50 g/m³ and 150 g/m³
- Tank pressure: 2 bar
- Valve opening time: 50 ms
- Total filtration area: 0.09 m^2 for flat media test rig and 0.65 m^2 for cylindrical-based set-up
- Pulsing at 1000 Pa differential pressure drop

Testing sequence:

- Conditioning 30 cycles, cleaning pulse at 1000 Pa.

Table 1 — Material specifications

Material	Fabric mass g/m²	Thickness mm	Air permeability m³/m²/min	Fibre length, mm	Blend ratio, %	Punches per cm²
Polytetrafluoroethylene (PTFE) coated filter media	520	2.3	8	51	100% PET	450
Stainless steel fibre blended with polyethylene terephthalate (PET) media	518	2.3	15	51	60% PET with 40% stainless steel fibre	450
Stainless steel fibre scrim media	505	2.1	12	51	5% stainless steel fibre in the scrim with 95% PET fibre	450

- Ageing 2500 cycles with a cleaning cycle at 20 s.
- Stabilising 10 cycles, cleaning pulse at 1000 Pa
- Measuring for 2 h at 1000 Pa (pressure-based cleaning)

The raw dust distribution of fly ash used for filter media characterisation is uniform.

3 Results and Discussion

Tables 2 and 3 present the average values of the filtration parameters for all investigated materials on a pilot pulse-jet filter unit at lower (50 g/m^3) and higher (150 g/m^3) dust concentrations, respectively. It is observed that the absolute filtration behaviour for each material is consistent with the results obtained from the flat-based test rig (Tables 3 and 4). However, this study primarily discusses the relative behaviour between the two test rigs. Table 4 shows the F-values at a 95% confidence level for all the parameters, revealing that for each factor, the calculated F-value is greater than the tabulated value. Table 5 summarises the contribution of each factor, viz. charge, material, dust concentration, and their interactions, in determining the filtration behaviour of the three materials. The findings indicate that while all factors significantly influence filtration performance, the effect of charge is the most pronounced in both test rigs, followed by material type and its interaction with charge. Conversely, dust concentration exhibits the least influence, primarily due to dust agglomeration facilitated by pre-charge, which enhances the dust cake properties and prevents particulate penetration into the inner layer of the filter media. These results highlight that pre-charge levels and media structure govern the movement of dust on the filter media. Additionally, the regression equations and correlation coefficients (r) for each response are found to be statistically significant and within an acceptable fit.

Table 2 — Material performance on pilot pulse jet filter unit under different charge levels at 50 g/m^3 dust concentration

Response	PTFE coated filter media				Stainless steel fibre blended with PET media				Stainless steel fibre scrim media			
	Dust charge level											
	0 kV	4 kV	8 kV	12 kV	0 kV	4 kV	8 kV	12 kV	0 kV	4 kV	8 kV	12 kV
$PM_{2.5}$ (µg/m³)	1021	841	715	671	1236	901	802	747	1339	1075	908	849 849
PM_{10} (µg/m³)	1409	1231	1189	1146	1581	1386	1277	1249	1759	1518	1406	1372
Mass conc. (mg/m³)	1.87	1.61	1.46	1.39	1.98	1.73	1.52	1.47	2.16	1.88	1.72	1.59
Particle no. conc. (P/cm³)	4341	3367	2931	2832	5103	4015	3493	3343	5764	4506	4014	3727
D_{10} (µm)	1.03	1.30	1.41	1.98	1.00	1.18	1.28	1.71	0.86	1.00	1.17	1.56
D_{50} (µm)	1.43	1.90	2.03	2.17	1.32	1.51	1.92	2.01	1.22	1.33	1.73	1.90
D_{90} (µm)	2.67	2.99	3.07	3.37	2.47	2.89	3.11	3.15	2.01	2.52	2.88	3.00
Residual pressure drop (Pa)	613	517	496	471	661	592	551	525	718	647	599	561

Table 3 — Material performance on pilot pulse jet filter unit under different charge levels at 150 g/m^3 dust concentration

Response	PTFE coated filter media				Stainless steel fibre blended with PET media				Stainless steel fibre scrim media			
	Dust charge level											
	0 kV	4 kV	8 kV	12 kV	0 kV	4 kV	8 kV	12 kV	0 kV	4 kV	8 kV	12 kV
$PM_{2.5}$ (µg/m³)	1287	1083	945	896	1482	1236	1086	1001	1694	1379	1219	1122
PM_{10} (µg/m³)	1720	1501	1396	1358	1901	1658	1539	1468	2089	1831	1676	1584
Mass conc. (mg/m³)	1.96	1.62	1.43	1.51	2.09	1.82	1.64	1.53	2.28	2.06	1.80	1.65
Particle no. conc. (P/cm³)	5523	4190	3828	3628	6208	5182	4382	4094	6967	5819	5089	4648
D_{10} (µm)	0.89	1.08	1.19	1.72	0.71	0.80	0.99	1.47	0.64	0.78	0.93	1.26
D_{50} (µm)	1.29	1.75	1.55	1.91	1.05	1.19	1.38	2.47	0.81	1.10	1.16	1.84
D_{90} (µm)	2.51	2.43	2.47	2.94	1.86	2.07	2.77	3.03	1.73	1.92	2.49	2.90
Residual pressure drop (Pa)	646	564	511	492	707	622	579	551	736	671	617	584

Table 4 — Calculated F-values for all parameters derived from three-way ANOVA

Filtration Parameter	Material		Charge		Dust conc.		Material × Charge		Charge × Dust Conc.		Dust Conc. × material	
	F_{table} = 2.87		F_{table} = 3.10		F_{table} = 4.35		F_{table} = 2.28		F_{table} = 3.10		F_{table} = 2.87	
	Flat	Pilot	Flat	Pilo	Flat	Pilot	Flat	Pilot	Flat	Pilot	Flat	Pilot
$PM_{2.5}$ (μg/m³)	89.57	73.42	102.1	115.3	71.8	62.47	92.18	77.31	63.52	69.27	81.03	59.06
PM_{10} (μg/m³)	109.7	117.8	133.8	156.6	57.31	48.21	97.13	71.21	51.03	61.31	66.31	70.09
Mass conc. (mg/m³)	81.41	70.16	91.03	99.34	52.08	55.56	72.49	56.28	49.07	63.17	72.13	62.65
Particle no. conc. (P/cm³)	87.31	7.38	99.05	131.7	39.81	33.11	65.05	58.11	43.21	31.18	57.05	51.23
D_{10} (μm)	47.08	41.28	62.07	53.11	47.14	58.72	37.17	43.31	53.18	45.03	61.26	50.29
D_{50} (μm)	40.28	49.29	57.14	63.61	51.27	38.86	29.57	33.11	42.23	36.34	39.34	31.07
D_{90} (μm)	58.17	67.92	50.26	68.09	59.11	39.79	29.17	35.16	53.72	47.39	55.92	47.71
Residual pressure drop (Pa)	97.37	118.31	147.3	181.2	70.42	89.64	101.5	84.3	69.13	51.52	79.09	62.81

Table 5 — Contribution percentage for all parameters derived from three-way ANOVA

Filtration Parameter	Material		Charge		Dust conc.		Material × Charge		Charge × Dust conc.		Dust conc.× Material	
	Flat	Pilot	Flat	Pilot	Flat	Pilot	Flat	Pilot	Flat	Pilot	Flat	Pilot
$PM_{2.5}$ (μg/m³)	21.34	20.49	25.64	26.85	10.06	13.09	21.14	17.17	17.64	15.72	11.57	13.73
PM_{10} (μg/m³)	18.26	22.11	23.06	26.07	15.31	11.38	23.56	19.53	17.23	10.52	10.51	7.48
Mass conc. (mg/m³)	16.83	20.27	20.07	24.79	19.71	16.81	22.17	17.37	17.83	12.61	12.61	8.26
Particle no. conc. (P/cm³)	17.16	22.45	21.47	27.18	10.81	15.96	23.17	18.03	13.86	13.16	13.16	7.41
D_{10} (μm)	15.13	18.64	23.63	27.72	17.64	16.51	14.18	8.82	10.37	11.39	11.37	8.78
D_{50} (μm)	17.56	20.81	22.8	21.71	14.18	17.29	9.46	10.23	13.61	10.93	13.49	9.91
D_{90} (μm)	18.16	20.72	24.81	21.55	15.22	16.5	8.94	11.29	12.17	10.82	10.52	7.79
Residual pressure drop (Pa)	22.09	20.78	20.31	24.16	10.28	18.09	21.79	17.47	17.43	10.75	14.02	8.21

3.1 Correlation Behavior of Emission-Related Parameters

Figure 1 illustrates $PM_{2.5}$ emissions for PTFE-coated media, stainless steel fibre blended with PET media, and stainless steel fibre scrim media. Among the three materials, PTFE-coated media exhibits the lowest particulate emissions in both test rigs, followed by stainless steel fibre blended with PET media and stainless steel fibre scrim media under both charged and uncharged conditions. However, particulate emissions are consistently higher in the pilot pulse-jet filter unit compared to the flat-based test rig across all charge levels and dust concentrations. This discrepancy can be attributed to differences in airflow regulation. In the flat-based test rig, air entry occurs from a single side, and the smaller height of the media facilitates relatively uniform airflow distribution. In contrast, the pilot filter media has a greater height and broader dimensions, resulting in non-uniform dust deposition due to unsteady airflow dynamics. The outer-to-inner airflow across the bag (pilot filter media) is highest near the collar and decreases along its length, leading to inevitable variations in dust deposition. Consequently, aerosols follow the path of least resistance, leading to inadequate dust cake formation in certain areas of the pilot media and resulting in higher emissions. Furthermore, gravitational effects may cause dust dislodgement from the pilot media prior to the cleaning cycle.

During the cleaning operation, inner-to-outer airflow is reduced at the top of the pilot media, which is in close proximity to the pulsing nozzless[10]. This results in intense shaking at the top, which diminishes along the length of the bag, leading to uneven cleaning efficiency. Despite these differences, a strong correlation between the emission values of the two test rigs is observed, with emissions consistently higher in the pilot filter unit (Fig. 2). The role of charge is significant in both test rigs, with a marginally greater effect in the pilot filter unit due to a higher number of inlet particles. The interaction between dust concentration and charge is also more prominent in the pilot filter

unit, likely due to the increased number of larger particles (>1 µm) in the flue gas, which amplifies the charge effect.

For PTFE-coated media, the charge has a lesser impact on downstream particulate emissions than stainless steel fibre blended with PET media and stainless steel fibre scrim media in both test rigs. This can be attributed to PTFE-coated media's inherently superior particle capture efficiency, even in the absence of charge. Consequently, the reduction in particulate emissions from 0 kV to 4 kV is relatively minor. In contrast, stainless steel fibre blended with PET media and stainless steel fibre scrim media exhibit greater particle seepage under uncharged conditions. However, under charged conditions, particle agglomeration at the pre-charged state prevents further penetration, resulting in a more pronounced improvement in filtration efficiency. Notably, the interaction between dust concentration and charge is more pronounced in the flat-based test rig due to more uniform dust deposition, enhancing the cumulative effect of these factors (Table 5).

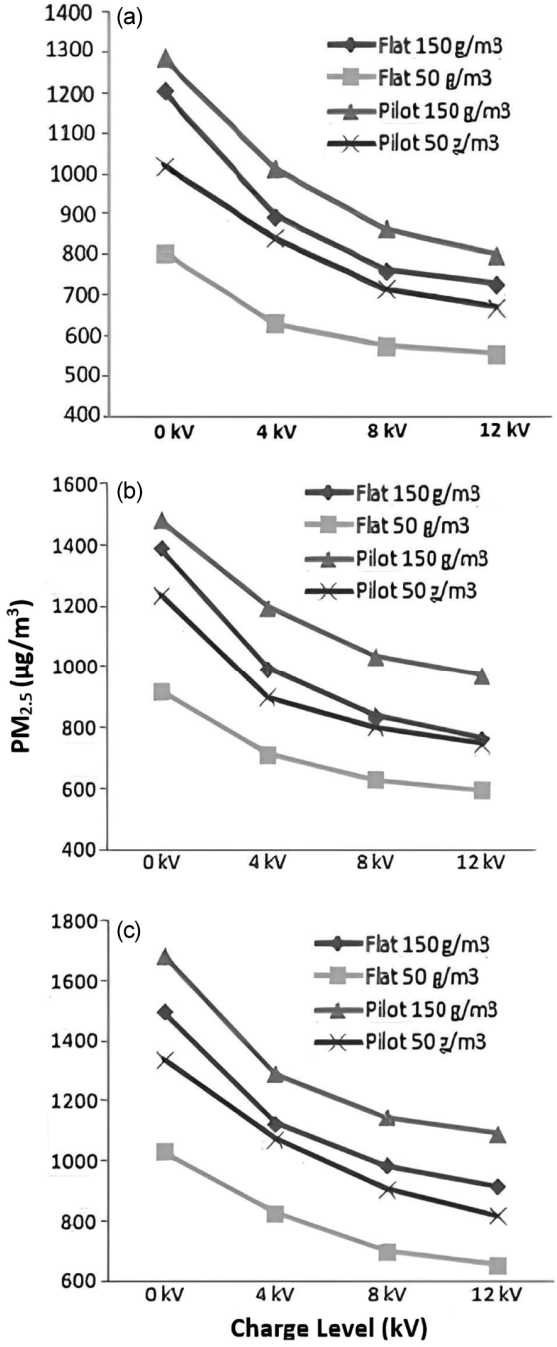

Fig. 1 — $PM_{2.5}$ emission behaviour for (a) PTFE-coated media, (b) stainless steel fibre blended with PET media and (c) stainless steel fibre scrim media

Figures 3 and 4 further illustrate that downstream mass and particle number concentrations exhibit strong correlations between the two test rigs. However, downstream particle number concentrations are consistently higher across all materials in the pilot filter unit. This trend aligns with particulate emissions, suggesting that variations in mass concentration and particle number concentration are influenced by the same factors. Under charged conditions, the capture efficiency for particles larger than 10 µm is greater in the flat-based test rig, as

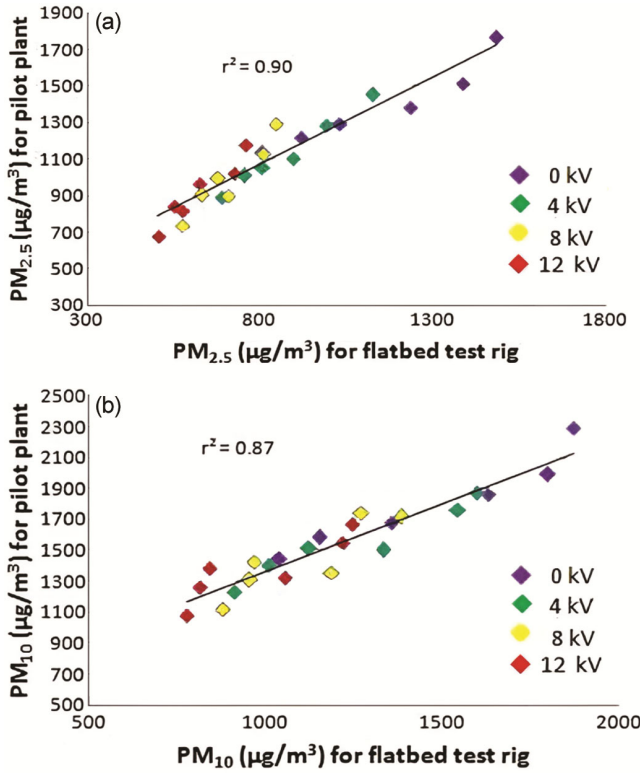

Fig. 2 — Correlation behaviour of emissions between flat and pilot test rigs for (a) $PM_{2.5}$ and (b) PM_{10}

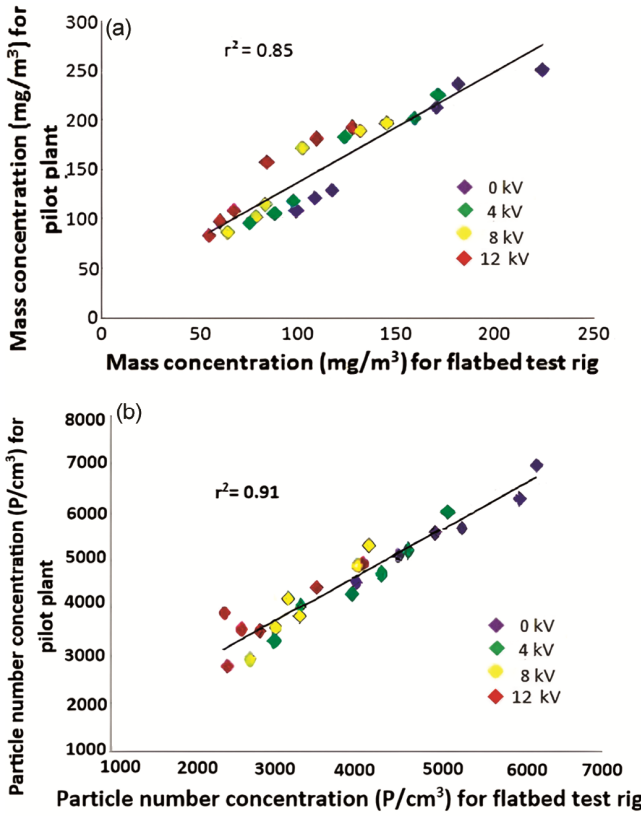

Fig. 3 — Correlation behaviour between flat and pilot test rigs for (a) downstream mass concentration and (b) particle number concentration

indicated by the smaller difference between total mass concentration and PM_{10} emission across all materials. This finding reinforces the significant role of charge in filtration performance, particularly in the pilot filter unit.

3.2 Charge Dissipation Behavior of Materials

Half-decay time tests indicate that materials with longer charge dissipation times exhibit lower particulate emissions. As charged particles accumulate on the media surface, charge dissipation leads to the gradual breakdown of agglomerated particles. A longer dissipation time suggests a slower breakdown, delaying particle penetration into the inner media layers and resulting in improved surface filtration.

Table 6 summarises charge dissipation test results. The dissipation time is shorter for stainless steel fibre blended with PET media compared to PTFE-coated media due to the presence of conductive stainless steel fibres, which facilitate charge dissipation. The dissipation time for stainless steel fibre scrim media is the shortest among the three materials due to the presence of conductive filaments arranged in a

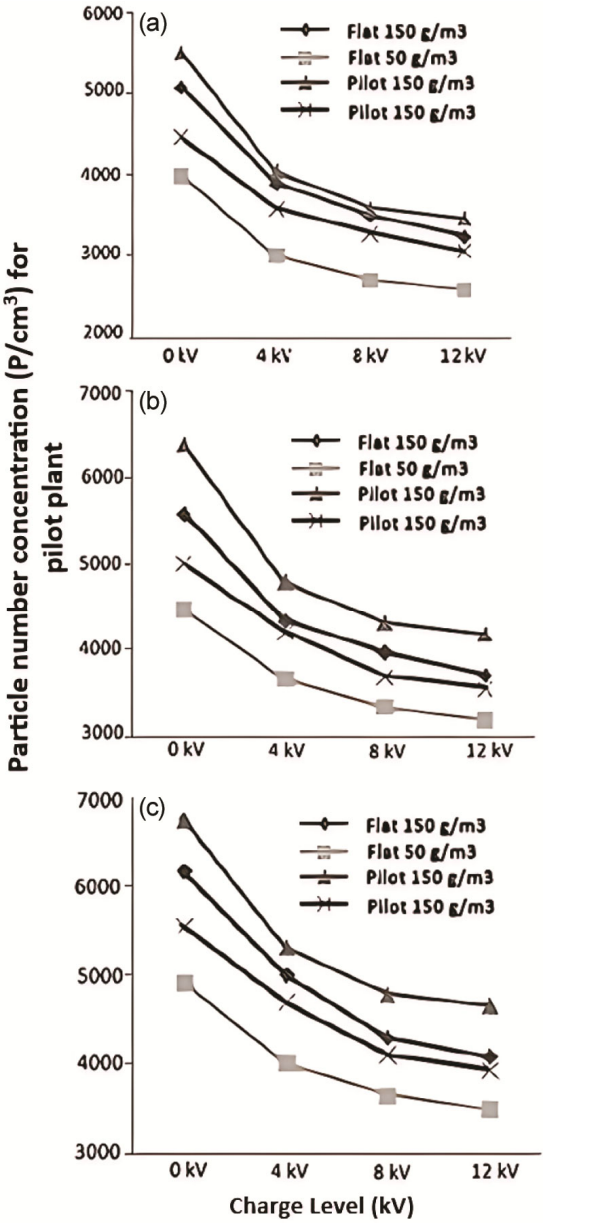

Fig. 4 — Particle number concentration behaviour for (a) PTFE-coated media, (b) stainless steel fibre blended with PET media and (c) stainless steel fibre scrim media

Table 6 — Charge dissipation test results

Material	Half-decay time (s)		
	4 kV	8 kV	12 kV
PTFE coated media	9.2	11.4	12.8
Stainless steel fibre blended with PET media	6.8	8.1	10.9
Stainless steel fibre scrim media	4.9	7.2	9.2

structured manner, providing a continuous path for charge dissipation. In contrast, other materials exhibit discrete charge dissipation paths, leading to relatively slower dissipation.

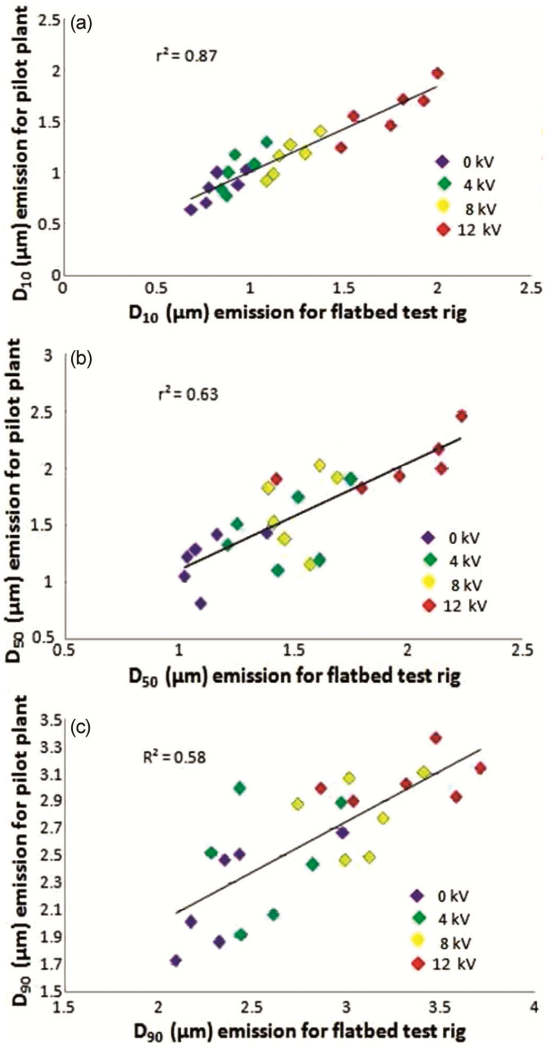

Fig. 5 — Correlation behaviour for downstream particle size distribution at (a) D_{10}, (b) D_{50}, and (c) D_{90}

3.3 Correlation Behaviour of Particle Size Distribution (D_{10}, D_{50}, D_{90})

Figure 5 illustrates the correlation between the two test rigs in terms of downstream particle size distribution (D_{10}, D_{50}, and D_{90}). While no distinct trend is observed, particle size distribution values generally increase with higher pre-charge levels (0 kV to 12 kV) in both test rigs. This is likely due to lower emissions at higher pre-charge levels, resulting in fewer particles of each size range in the downstream flow. Additionally, under charged conditions, the dust cake on the filter media surface also acquires charge, promoting particle agglomeration, which may further increase average particle size. Among the three particle size distribution parameters, charge exhibits the greatest influence on D_{90} in both test rigs, indicating that charge has a more pronounced effect on capturing larger particles. Furthermore, a strong interaction between charge and dust concentration is observed in both test rigs, reinforcing the role of charge in filtration efficiency.

4 Conclusion

This study highlights the significant role of charge, material type, and dust concentration in filtration performance across two test rigs. Charge exhibits the most substantial impact, enhancing filtration efficiency through particle agglomeration and dust cake formation. PTFE-coated media consistently outperforms the other materials in terms of particulate capture, while stainless steel fibre scrim media exhibits the fastest charge dissipation. The pilot pulse-jet filter unit demonstrates higher emissions and particle concentrations compared to the flat-based test rig due to its non-uniform dust deposition and cleaning dynamics. These findings provide valuable insights into optimising filtration efficiency and understanding the influence of electrostatic charge on different filter media.

References

1 Adamiak K, *J Electrost*, 71 (2013) 673, https://doi.org/10.1016/j.elstat.2013.03.001.
2 Adamiak K & Atten P, *IEEE Trans Dielect Electr Insul*, 16 (3) (2009) 608.
3 Carotenuto C, Natale F D & Lancia A, *J Chem Eng*, 165 (2010) 35. https://doi.org/10.1016/j.cej.2010.08.049.
4 Choi H J, Kumita M, Seto T, Inui Y, Bao L, Fujimoto T & Otani Y, *J Aero Sci*, 114 (2017) 244. https://doi.org/10.1016/j.jaerosci.2017.09.020.
5 Morawska L, Agranovski V, Ristovski Z & Jamriska M, *Indoor Air*, 12 (2002) 129.
6 Jaworek A, Sobczyk A T, Krupa A, Marchewicz A, Czech T & Śliwiński L, *Sep Purif Technol*, 213 (2019) 283.
7 Dutta S, Mukhopadhyay A, Choudhary A K & Reddy C C, *J Inst Eng (India) Ser E*, 99 (2) (2018) 219, https://doi.org/10.1007/s40034-018-0129-0.
8 Dunnett S J & Clement C F, *J Aero Sci*, 53 (2012) 85.
9 Wang F L, He Y L, Tang S Z, Kulacki F A & Tao Y B, *Fuel*, 237 (2019) 308.
10 Li J, Wu D, Wu Q & Luo M, *Sep Purif Technol*, 213 (2019) 101.
11 Dutta S, Mukhopadhyay A, Choudhary A K & Reddy C C, *J Indf Text*, 52 (2022) 1.
12 Dutta S, Mukhopadhyay A, Choudhary A K & Reddy C C, *J Inst Eng Ser E*, 100 (1) (2019) 47, https://doi.org/10.1007/s40034-019-00139-z.
13 Dutta S, Mukhopadhyay A, Choudhary A K & Reddy C C, *Indian J Fibre Text Res*, 46 (2021) 269.
14 Simon X, Bémer D, Chazelet S, Thomas D & Régnier R, *Powder Technol*, 201 (2010) 37.
15 Singh P, Mukhopadhyay A & Gupta P, *Powder Technol*, 426 (2023) 118614, https://doi.org/10.1016/j.powtec.2023.118614.